UDC 547.024

DENSITY FUNCTIONAL THEORY, DOCKING, SYNTHESIS AND BIOLOGICAL EVALUATION OF SOME 2-(2-ARYL AMINO) PHENYL ACETAMIDE DERIVATIVES

Karam S. Atrushi[1], Dana M. Ameen[2], Faris T. Abachi[3]*

[1]*Department of Pharmaceutical Chemistry, College of Pharmacy, University of Duhok.*
[2]*Department of Pharmaceutical Chemistry, College of Pharmacy, Hawler Medical University, Erbil.*
[3]*Department of Pharmacy, Al-Hadbaa University College, Mosul, Iraq.*
**Corresponding author: Faris_abachi@uomosul.edu.iq*

Received 22.02.2024
Accepted 27.05.2024

Abstract: *A series of new 2-(2-aryl amino) phenyl acetamide derivatives were synthesized and their chemical structures were identified using spectroscopic techniques (UV-VIS, FTIR, 1HNMR, and MS). Computational studies have been carried out for prediction reactivity and density function theory (DFT) calculations for the acetamide derivatives, as well as the spatial electron distribution of the highest occupied molecular orbital (HOMO) and lowest unoccupied molecular orbital (LUMO) were computed. The docking study against prostaglandin synthetase-2 (COX-II coenzyme) was computed, and four compounds (D, F, H, and L) gave high scores (Kcal/mol). Some of these synthetic compounds were evaluated for their biological activities in vitro (antimicrobial, antioxidant, anticancer, and anti-inflammatory). Finally, the compounds B, D, F, and K have a good correlation between theoretical and experimental studies as cyclooxygenase inhibitors and weak to moderate antimicrobial, antioxidant, and cancer activities.*

Keywords: *COX-II inhibitors, DFT, Anticancer, HOMO, Acetamide derivatives.*
DOI: 10.32737/2221-8688-2024-4-389-401

1. Introduction

The nonsteroidal anti-inflammatory drugs [NSAIDs] are a group of chemically dissimilar agents that differ in their therapeutic actions. Nearly, all NSAIDs have greater selectivity for COX-I as analgesics [1]. There unwanted side effect of causing gastric damage is ascribed to the inhibition of COX-I, resulting in an inability to COX-II inhibitor [2].

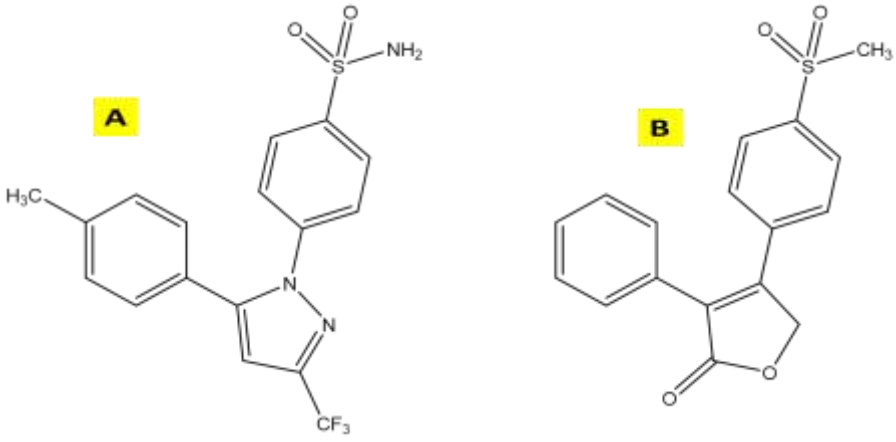

Fig. 1. A representative structure of (A) celecoxib and (B) Rofecoxib with functional groups

The first COX-II inhibitor, celecoxib was approved in the United States in 1998, and rofecoxib was approved in 1999 (Fig. 1).

The broad spectrum activities of COX-II inhibitors in the development of colon cancer, and also with inflammatory processes in the brain that appear to be involved in the development of Alzheimer's disease [3]. The prostaglandins (PGs) are a group of naturally occurring compounds whose molecule structures are based on that of prostanoic acid [4]. They were believed to be synthesized in the prostate glands in addition to rheumatoid arthritis and osteoarthritis [5]. Also, COX-II inhibitor drugs play a major role in colorectal carcinogenesis [6]. Cyclooxygenase-II or COX-II is the enzyme responsible for the synthesis of prostanoids from arachidonic acid [4]. Besides its role in inflammation, it is currently under study for a role in cancer and cardiovascular diseases [7].

Recently, new diclofenac derivatives have been prepared and exhibited no toxicity, and the preservation of stomach wall mucus may be the cause of the gastroprotective effect[8]. In this study, eight new 2-(2-aryl amino) phenyl acetamide derivatives have been designed, to predict the theoretical density function theory (DFT), docking, synthesis, characterization and evaluation of the biological activities. Our research aims to develop a straightforward and cost-effective synthetic method for creating novel 2-(2-aryl amino) phenyl acetamide derivatives, which hold potential in various pharmaceutical applications. By leveraging the principles of density functional theory (DFT) for *in silico* studies, we can accurately predict and optimize the electronic structures and properties of these derivatives before embarking on laboratory synthesis. DFT allows us to understand the molecular orbitals, electron density distribution, and reactivity patterns of our target compounds, facilitating the rational design of synthetic routes that minimize costs and maximize yield. Our method involves strategic selection of starting materials and catalysts to streamline reaction steps while ensuring high purity and desired functionalization of the acetamide core.

2. Experimental part

2.1. Materials

All chemicals used in the synthesis were purchased from Aldrich Chemical Co (Germany). Melting points were recorded with an electrothermal melting point apparatus. Ultraviolet-visible spectra were recorded on T60 PG Instruments visible spectrophotometer (UK). FTIR spectra were recorded on a Shimadzu (Japan). ^{1}H-NMRspectra were measured on a JEOL JNM-ECZ400S 400 MHz NMR spectrometer (Japan). NMR solution of the obtained sample was prepared under deuterated chloroform ($CDCl_3$ Merck, Merck, D_2O Merck). ^{1}H-NMR spectra were scanned in the range of 0–20 ppm. All compounds were measured with D_2O exchange with NH, or OH groups. The LC/Q-TOF/MS system is considered of an Agilent 1290 Infinity LC system coupled with Agilent 6530 Accurate-Mass Quadrupole Time-of-Flight (Q-TOF) mass spectrometer (Agilent, USA).

2.2. Theoretical calculations

Density functional theory (DFT): The chemical structures of anthranilic acid derivatives and their models have been drawn, using two- dimensional Chemdraw ultra version 11.0. Each molecular structure has been transferred to undergo a systematic energy minimization, using Chem 3D-ChemBioOffice software version 16.0.0.82 (level: Ultra). To reach the global minima, the optimization was started from molecular mechanics calculations MM2, and then MMFF94 methods were used to get a value smaller than 0.1 kcal/ mole of the root mean square (RMS) gradient [9]. The minimization process was continued, using semi-empirical calculations, including Austin Model number 1 (AM1), followed by Parameterized Model number 3 (PM3) methods to reach a negative sign of heat of formation, and a positive sign of frequency[10]. For density functional theory (DFT) calculations, the energy minimizations were continued, using DFT at the B3LYP level with a 6-311G basis set, until the minimum RMS gradient of 0.1 was

reached [10]. The estimations of descriptors were carried out by Gaussian 03w software, using DFT, Hartree–Fock ab initio (HF), and PM3 methods (closed-shell MOs), depending on the type of selected descriptor [11].

Molecular Docking: For molecular docking computation, Mcule docking online was used to predict the specific interactions between the ligand (compounds 1–8) and target proteins, including their binding affinities (Prostaglandin G_H synthetase). The ligand-protein complex was created and predicted the protein's active location where the ligand is in its optimal shape. The Discovery Studio Visualizer software 2021 was used to extract and display the ligand-protein interactions [11].

2.3. LC/Q-TOF/MS

The LC/Q-TOF/MS system is considered an Agilent 1290 Infinity LC system coupled with Agilent 6530 Accurate-Mass Quadrupole Time-of-Flight (Q-TOF) mass spectrometer (Agilent, USA) and ZORBAX RRHD Eclipse Plus C18, 95Å, 2.1 x 100 mm, 1.8 µm (Agilent, USA). The mobile phase system consisted of % 0.1 formic acid in water (A) and acetonitrile (B) using a gradient elution as follows: A mobile phase flow rate of 0.4 mL/min was employed for gradient elution at total 12-min run time as follows: 0–0.5 min, 2% B; 0.5–4 min, 20% B; 4–8 min, 50% B; 4–6 min, 95% B; 8–9 min, 95% B; 9-9.25 min 2 % B and 9.25-12 min, 2% B for equilibration of the column. The column temperature was set to 55 °C during the analysis. The injection volume was 4.0 µL. The positive ion scan mode at 3.5-kV capillary voltage was applied during the study. Mass scanning was ranged from 50 to 1000 m/z. The ion source was Electron Spray Ionization (ESI). MS absorbance threshold was set at 200. The instrument acquired data by optimized parameters such as drying gas temperature, 350 °C; drying gas flow, 11 L/min; nebulizer, 40 psi; sheath gas temperature, 350 °C; sheath gas flow, 11 L/min [12].

2.4. General procedures for the synthesis of amide derivatives (A-K) (13)

Substituted phenylacetic acid (1 mmol), and thionyl chloride (2.0 g, 0.02 mol) were dissolved in chloroform (20 mL) to form acid chloride derivatives.

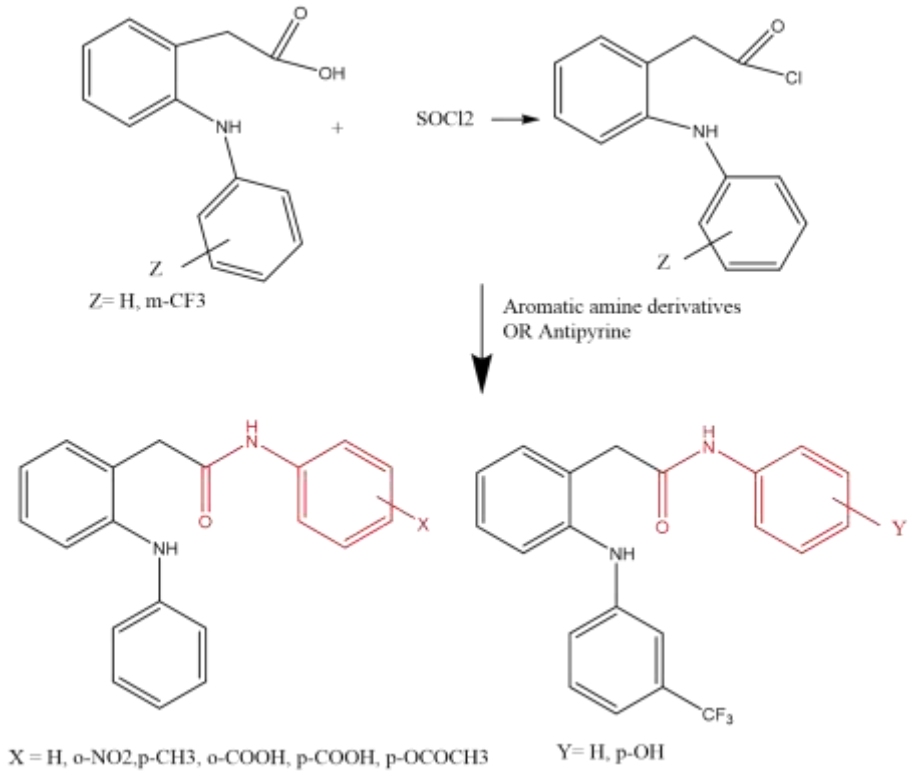

Fig. 2. Reaction pathway for the synthesis of the acetamide derivatives.

The mixture was stirred in the presence of pyridine (2.78 ml, 0.02 mmol) at 0° C, and the appropriate aromatic amine derivatives or antipyrine (2 mmol) was added, then the mixture was refluxed for 3h. The solvent was evaporated under a vacuum. The semisolid organic layer was washed with saturated sodium bicarbonate solution and extracted with ether, dried and concentrated under reduced pressure. The resultant crude residue was crystallized (Fig. 2).

Greenish Powder, yield 90 %, m.p. 190d ° C, R_f:0.78, M.F: $C_{20}H_{18}N_2O$, UV. λ_{max}: 255 nm IR ν_{cm-1}: 3234.20, 3069.21, 2948.48, 1666.73, 1467.12, 1384.70, 1227, ^{1}HNMR ($CDCl_3$) δppm: 4.65 (m,1H) HOD, 4.80 (s, 2H) CH_2, 7.17-8.56) (m,14H) three phenyl rings, LC-MS, m/z: 302

Compound B: (N-(2-nitrophenyl)-2-(2-(phenylamino) phenyl) acetamide) Yellowish Powder, yield 88%, m.p. 132-134 °C, R_f: 0.64, UV. λ_{max}: 256 nm, IR ν_{cm-1}: 3127.59, 3067.38, 2889.25, 1660.65, 1312.48, ^{1}HNMR ($CDCl_3$)) δppm: 4.65 (m,1H) HOD, 4.80 (s, 2H) CH_2, 7.84-8.58 (m,13H) 3phenyl rings, LC-MS, m/z: 347

Compound C: (2-(2-(phenylamino)phenyl)-N-(p-tolyl)acetamide)
White Powder, yield 84 %, m.p. 185d°C, R_f : 0.75 ,M.F: $C_{21}H_{20}N_2O$, UV. λ_{max}: 255 nm IR ν_{cm-1}: 3138.56, 3068, 2944.93, 1684.75,1684.75, 1608.63, ^{1}HNMR ($CDCl_3$) δppm): 2.13 (s, 3H) CH_3, 4.65 (m,1H) HOD, 4.80 (s,2H) CH_2, 7.04-7.13 (dd, 4H) para-substituted phenyl ring, 7.89- 8.57 (m, 9H) two phenyl rings, LC-MS, m/z: 316

Compound D: (N-(1,5-dimethyl-3-oxo-2-phenyl-2,3-dihydro-1H-pyrazole-4-yl)-2-(2-(phenylamino) phenyl) acetamide)

Orange Powder, yield 71%, m.p. 152d °C, R_f: 0.52, M.F: C_{25} $H_{24}N_4O_2$, UV. λ_{max}: 255 nm, IR ν_{cm-1}: ^{1}HNMR ($CDCl_3$) δppm: 3.08 (m, 6H) 2 CH_3, 4.65 (m, 1H) HOD, 4.80 (d, 2H) CH_2, 7.16-8.58 (m,14) three phenyl rings, LC-MS, m/z: 412

Compound E (2-(2-(2-(phenylamino) phenyl) acetamido) benzoic acid)
Purple Powder, yield 91%, m.p. 145d °C, R_f: 0.59, M.F: $C_{21}H_{18}N_2O_3$, UV. λ_{max}: 255 nm, IR ν_{cm-1}: 3235.16, 3066.56, 2922.23, 1641.76, 1545.99, 1480.13, 1052.20, ^{1}HNMR ($CDCl_3$) δppm: 4.65 (m, 1H) HOD, 4.80 (s,2H) CH_2, 7.08- 8.57 (m, 13H) three phenyl rings, LC-MS, m/z: 346

Compound F (4-(2-(2-(phenylamino) phenyl) acetamido) benzoic acid)
White Powder, yield 91%, m.p. 155-157 °C, R_f: 0.68, M.F: $C_{21}H_{18}N_2O_3$, UV. λ_{max}: 227, 255, 284 nm, IR ν_{cm-1}: 3201.50, ^{1}HNMR ($CDCl_3$ δppm): 4.65 (m, 1H) HOD, 4.80 (s,2H), 7.08- 7.83 (dd, 4H) para-substituted phenyl ring, 7.85- 8.57 (m, 9H) two phenyl rings, LC-MS, m/z: 346

Compound G: (methyl 4-aminobenzoate)
Grey Powder, yield 68%, m.p. 110-112 °C, R_f:0.42 , M.F: $C_8H_9NO_2$, UV. λ_{max}: 264 nm, IR ν_{cm-1}:3286.55, 3140.42, 3076.02, 1747.44, 1662.28, 1548.88, 1196.27, ^{1}HNMR ($CDCl_3$ δppm): 2.27 (s,3H) CH_3, 6.98-7.58 (dd, 4H) araomatic, 7.56 (br, 2H) NH_2, LC-MS, m/z: 151.

Compound H: (methyl 4-(2-(2-(phenylamino)phenyl)acetamido)benzoate)
Violet Powder, yield 73%, m.p. 105-107 ° C, R_f: 0.49, M.F: $C_{22}H_{20}$ N_2O_2, UV. λ_{max}: 255 nm, IR ν_{cm-1}: 3198.79, 3056.12, 2944.38, 1670.06, 1526. 42, 1103.32, ^{1}HNMR ($CDCl_3$) δppm: 1.85 (s,3H) CH3, 4.5 (s, 2H) CH2, 4.65 (m,1H) HOD, 7.8-8.2(m, 9H) two phenyl rings, 8.2-8.5 (dd, 4H) para substituted phenyl ring. LC-MS, m/z: 360

Compound J: (2-(2-((3-(trifluoromethyl) phenyl) amino) phenyl) acetic acid)
Gray Powder, yield 40 %, m.p. 124d ° C, R_f:0.66, M.F: $C_{15}H_{12}F_3NO_2$, UV. λ_{max}: 231nm, IR ν_{cm-1} : 3198. 24, 3067.16, 2948.62, 1687.21, 1610.56, 1467. 48, 1383. 62, 1231. 57, ^{1}HNMR ($CDCl_3$) δppm: 3.31 (s, 2H) CH_2, 4.65 (m, 2H) HOD, 6.74-7.09 (m, 8H) two phenyl rings, LC-MS, m/z: 295

Compound K: (N-phenyl-2-(2-((3-(trifluoromethyl) phenyl) amino) phenyl) acetamide)
Orange Powder, yield 86%, m.p. 135d °C, R_f:0.77, M.F: $C_{21}H_{17}F_3N_2O$, UV. λ_{max}: 233, 255 nm , IR ν_{cm-1} : 3219.80, 1640.01, 1564.83, 1102.69, ^{1}HNMR ($CDCl_3$) δppm: 4.65 (m,1H) HOD, 4.80 (d, 2H) CH_2, 7.16- 8.57 (m, 13H) three phenyl rings LC-MS, m/z: 370

Compound L: (N-(4-hydroxyphenyl)-2-(2-((3-(trifluoromethyl) phenyl) amino) phenyl) acetamide)

Gray Powder, yield 69%, m.p. 130d °C, R_f:0.45, M.F: $C_{21}H_{17}F_3N_2O_2$, UV. λ_{max}: 256 nm, IR ν_{cm-1}: 3410.15, 3174.36,3056.13, 1676.40, ^{1}HNMR ($CDCl_3$) δppm: 4.65 (m, 2H) HOD, 4.80 (s,2H) CH2, 6.75-7.20 (dd, 4H) para-substituted phenyl ring, 7.80-8.65 (m, 8H) two phenyl rings, LC-MS, m/z: 386

2.5. Biological studies

2.5.1. Antioxidants of some synthetic compounds (*in vitro*)

Diphenyl-2-picrylhydrazyl Free Radical Scavenging Activity test [14]: The free radical scavenging activity of each sample was measured according to Lee, *et al.* [15] as follows: known volumes (50, 100, 150 μL) of each sample were individually added to test tubes then completed to a known volume (1.0ml) by D.W, (1.0ml) of DPPH solution (0.2 mL in ethanol) was added to each tube then mixed well and incubated at room temperature for 30 min. The control was prepared by the same procedure without phenolic pyrimidine derivatives. Ascorbic acid solution (0.03 % w/v) was used as a positive control. The absorbance (A) of the solution was measured at 517nm using a T60 PG Instruments visible spectrophotometer [UK]. The inhibition DPPH free radical in present (I %) was calculated from the following equation. I %=[(Ac-As)/Ac]·100.

2.5.2. Antimicrobial assay

Antimicrobial screening of the synthesized compounds was performed by CO-ADD (The Community for Antimicrobial Drug Discovery), funded by the Wellcome Trust (UK) and The University of Queensland (Australia) [15-20]. The antimicrobial activity was examined against some representative fungi and bacteria as given within the main text at 32 $mg{\cdot}mL^{-1}$ according to standard broth microdilution assays [9]. For toxic compounds, a follow-up hit confirmation was triggered, where the toxicity was established by employing a dose–response assay against the same microbe strain. No animals were used in this study. Cell lines (bacteria, fungi, mammalian) were sourced from the American Type Culture Collection (ATCC) and were approved by The University of Queensland Institutional Human Research Ethics Committee, Approval Number 2014000031. The protocol of the antimicrobial testing in this centre (CO-ADD), Australia, was as follows:

2.5.2.1. Antibacterial assay (16):

All bacteria, *S. aureus* (Sa) (Strain ATCC 43300, MRSA), *E. coli* (Ec) (Strain ATCC 25922, FDA control strain), *K. pneumoniae* (Kp) (Strain ATCC 700603, MDR), *A. baumannii* (Ab) (Strain ATCC 19606, Type strain), *P. aeruginosa* (Pa) (Strain ATCC 27853, Quality control strain), were cultured in Cation-adjusted Mueller Hinton **b**roth (CAMHB) at 37 °C overnight. A sample of each culture was then diluted 40-fold in fresh broth and incubated at 37 °C for 1.5–3 h. The resultant mid-log phase cultures were diluted (CFU/mL measured by OD_{600}), and then added to each well of the compound-containing plates, giving a cell density of 5×10^5 CFU/mL and a total volume of 50 μL. All the plates were covered and incubated at 37 °C for 18 h without shaking.

2.5.2.2. Antifungal Assay [17-20]

Fungi strain *C. albicans* (Ca) (Strain ATCC 90028, CLSI reference) and *C. neoformans* (Cn) (Strain ATCC 208821, H99 Type strain), were cultured for 3 days on Yeast Extract-Peptone Dextrose (YPD) agar at 30 °C. A yeast suspension of 1×10^6 to 5×10^6 CFU/mL (as determined by OD_{530}) was prepared from five colonies. The suspension was subsequently diluted and added to each well of the compound-containing plates giving a final cell density of fungi suspension of 2.5×10^3 CFU/mL and a total volume of 50 μL. All plates were covered and incubated at 35 °C for 36 h without shaking.

2.5.3. Anticancer activity [NCI-60 Screening Methodology (NCI, USA) [21]

Four compounds were submitted to the National Cancer Institute (NCI) and were screened on NCI 60 cell lines initially at a single high dose (10^{-5} M) on leukaemia, melanoma, lung, colon, CNS, ovarian, renal, prostate, and breast cancers cell lines. The one-dose data were reported as a mean graph of the percent growth (GP) of treated cells. The number reported for the one-dose assay is growth relative to the no-drug control and relative to the time-zero number of cells. The anticancer screening was carried out as per the NCI US protocol reported elsewhere [21]. We have discussed the anticancer screening method in

the present study based on a previously described method by Monks et al. [22].

2.5.4. Interpretation of One-Dose Data (NCI protocol, USA) [23, 24]

The One-dose data will be reported as a mean graph of the percent growth of treated cells and will be similar in appearance to mean graphs from the 5-dose assay. The number reported for the One-dose assay is growth relative to the no-drug control, and relative to the time-zero number of cells. This allows the detection of both growth inhibition (values between 0 and 100) and lethality (values less than 0). This is the same as for the 5-dose assay, described below. For example, a value of 100 means no growth inhibition. A value of 40 would mean 60% growth inhibition. A value of 0 means no net growth throughout the experiment. A value of -40 would mean 40% lethality. A value of -100 means all cells are dead. Information from the One-dose mean graph is available for comparison analysis.

3. Results and discussion

The most common method of experimental research is the computational quantum mechanical modeling method used in medicinal chemistry, this technique used to calculate the electronic structure of molecules including the optimized geometry, HOMO-LOMO and MEP, were made visible [21]. The ionization potential (I), electronic affinity (A), hardness (η), softness (σ), chemical potential (μ), electronegativity (χ), and electrophilicity (ω) (Table 1, Fig. 3).

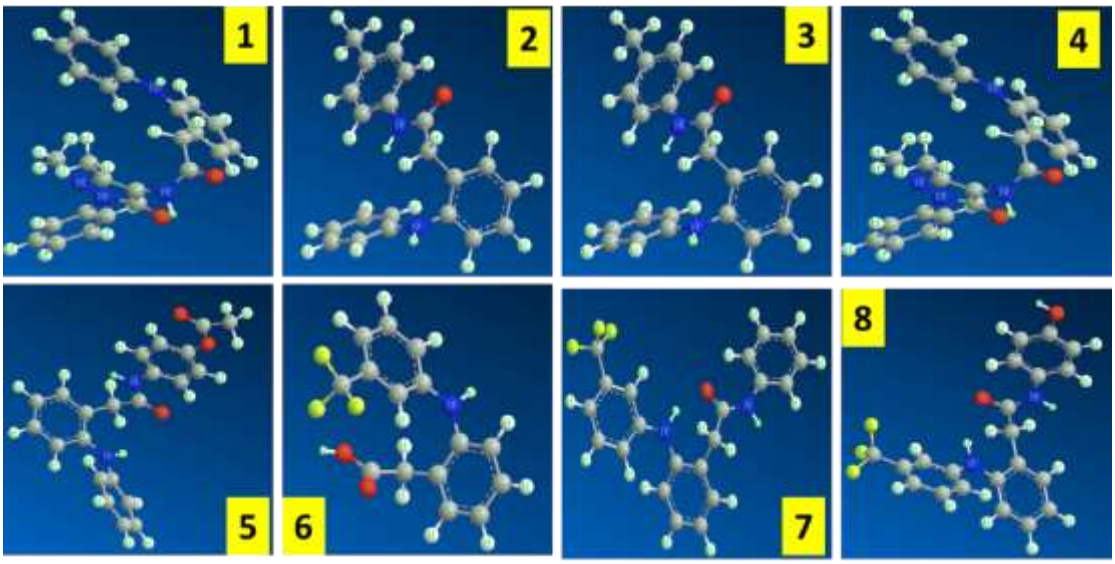

Fig. 3. 3-D molecular structures of 8 compounds after DFT (6-311G) minimization.

Table 1. Theoretical calculation of HOMO and LOMO energies of eight compounds.

ID	HOMO (eV)	LUMO (eV)	GAP (Δ E)	ionization potential (I)	electron affinity (A)	chemical potential (μ)	hardness (η)	softness (S)	Electrone gativity (x)	Electrophi licity (ω)
1 (D)	-0.19046	-0.02993	0.16053	0.19046	0.02993	-0.110195	0.080265	12.4587	0.110195	0.075643
2 (A)	-0.18251	-0.02154	0.16097	0.18251	0.02154	-0.102025	0.080485	12.4247	0.102025	0.064665
3 (C)	-0.20429	-0.01316	0.19113	0.20429	0.01316	-0.108725	0.095565	10.4641	0.108725	0.061849
4 (F)	-0.20711	-0.04988	0.15723	0.20711	0.04988	-0.128495	0.078615	12.7202	0.128495	0.105012
5 (H)	-0.19306	-0.02226	0.17080	0.19306	0.02226	-0.107660	0.085400	11.7096	0.107660	0.067861

6 (J)	-0.21657	-0.03185	0.18472	0.21657	0.03185	-0.124210	0.092360	10.8272	0.124210	0.083522
7 (K)	-0.20380	-0.02839	0.17541	0.20380	0.02839	-0.116095	0.087705	11.4019	0.116095	0.076837
8 (L)	-0.21372	-0.03131	0.18241	0.21372	0.03131	-0.122515	0.091205	10.9643	0.122515	0.082287
GAP (ΔE)= ELUMO-EHOMO; I= -EHOMO; A= -ELOMO; η= I- A^2; σ= I . η; X= I-A^2; μ=-x; ω= X^2.2η.; Electronic volt; eV.										

The Mcule molecular docking online was used to predict the interactions between the ligand (eight compounds and Celecoxib(Reference) and target protein (Prostaglandin G_H synthetase) were successfully recorded to their crystallography data. The RMSD values of these ligands compared to their original using Discovery Studio visualization software 2021 with DS visualizer [22] (Table 2).

Table 2. Docking of the 2-(2-aryl amino) phenyl acetamide derivatives

Letter	Compound No.	Score of binding prostaglandin G_H synthetase(Kcal/mole)
A	1	-7.2
B	2	-6.4
C	3	-
D	4	-8.0
E	5	-6.1
F	6	-9.2
G	7	-
H	8	-
J	9	-
K	10	-10.1
L	11	-9.1
	Celecoxib (Reference)	-10.4

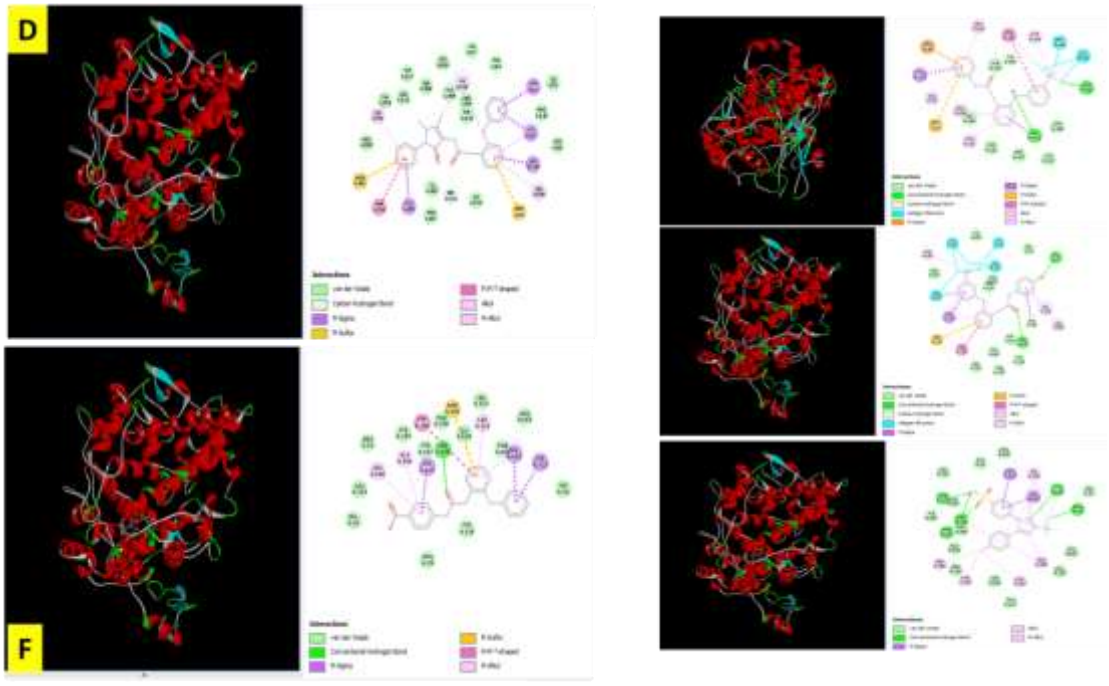

Fig. 4. 2-D and 3-D structures of the compounds K, L, and Celecoxib.

The docking studies have been done to elucidate the type of binding mode of the eight synthetic substituted phenyl acetamide derivatives and give the scores (Kcal/mole) with the specific target for COX-II enzyme, and the RMSD values were found to be less the 2 which gives the validity of the results of these docking [23].

Generally, the analysis of the docking results of these compounds has similar functional groups for the eight synthetic compounds, the interactions between amide, phenolic OH, secondary amine, trifluoromethyl group, phenyl functional groups, and active site of amino acids of the prostaglandin G_H synthetase (Figure 2). The 2D structures explain the types of many hydrophobic interactions (pi-sigma, amide –pi, between the ligand and the designated beside the hydrogen bonding, the most common amino acids are Ala 496 for pi-sigm, Met 491 for pi-sulfur, besides Leu 328, Ser 322, Phe 487, and Tyr 324 (Fig. 4).

The scoping study of the antimicrobial activity at CO-ADD using the minimum inhibitory concentration (MIC) (Table 4). Only four compounds were used for the preliminary test. Two compounds Dand H acetamide derivatives and two of fluorinated acetamide derivatives compounds K and L. Only compound D showed poor activity against the bacteria Ab MIC 83.02(μg/mL) as shown in Table 4 [24].

The *in vitro* assay of the antioxidant activity of four synthetic compounds was tested and evaluating scavenger activity of aqueous samples using the DPPH method and ascorbic acid as a reference. Antioxidant activity was carried out in triplicate [25]. The compounds D and L show weak to moderate antioxidant activity as compared to the standard (Table 3).

Table 3. Preliminary antimicrobial tests for synthetic compounds according to the CO-ADD protocols, the minimum inhibitory concentration(MIC) in (μg/mL) of the 4 synthetic compounds.

Compd No.	Sa	Ec	Kp	Pa	Ab	Ca	Cn	ID Compd* (32 ug/mL)	Ab 19606
D	3.35	-3.75	21.06	-0.44	38.22	7.45	-	C120404	38.22
H	-1.22	-4.54	11.75	1.07	15.49	19.33	-	C120405	15.49
K	6.42	-4.98	11.37	2.35	12.75	3.51	-	C120402	12.75
L	-0.57	-7.93	7.19	-1.84	28.77	10.45	-	C120403	28.77
* All are inactive agents except compound C120404 weak activity toward G(-: bacteria. Five types of bacteria are Sa: ATCC 43300, Ec: ATCC 25922, Kp: ATCC 700603, Pa: ATCC 27853, Ab: ATCC 19606, and Vancomycin. HCl, and Colistin sulfate as references. Two types of fungi (Yeast)are Ca: ATCC 90028, Cn: H99; ATCC 208821, and Fluconazole as a reference.									

Table 4. Scavenging activity of (aqueous samples) and Ascorbic acid against DPPH radical

Sample (OPEs)	Conc. (ppm)	Scavenging activity (%)
Aqueous sample D	500	50.1
	1000	76.9
	1500	80.5
Aqueous sample F	500	23.23
	1000	28.61
	1500	32.92
Aqueous sample J	250	28.15
	500	36.76
	750	54.0
Aqueous sample L	500	36.92
	1000	46.30
	1500	51.23
Ascorbic acid (standard)	7.5	92.6
	15	92.9

	23	95.5

Table 5. Anticancer test of the compounds (D, H, K, and L).

Compound ID	NSC	Growth (PW) %
D	845042/1	Melanoma 25.08 Ovarian 22.71
H	845043/1	Non-small cell lung cancer cell 28.67
K	845045/1	Melanoma 25.67 Non-small cell lung cancer cell 22.57
L	845044/1	Non-small cell lung cancer cell 16.98

Moreover, the percentage growth we used to study the cytotoxic activity of the 4 synthetic compounds by using 60 types of cancer cells is listed their activities in Table 5. Compound D (NSC 845042/1) showed inhibition activity agonists in two types of cancer cells melanoma and ovarian, while compound H (NSC 845043/1) showed inhibition activity against only non-small cell lung cancer, and similar results for compounds Kand L (NSC: 845045 and NSC 845044), respectively [25, 26].

In-vitro **Cyclooxygenase(COX) Inhibition Assay**

The selected synthesized compounds were accomplished there *in-vitro* COX-II inhibition assay by a previously reported method using an enzyme immune assay (EIA) kit [27]. The absorption of diverse yellow colours was measured by a UV-visible spectrophotometer (EI 2371**)** at λ 412 nm. The intensity of the yellow colour depends on the enzymatic reaction which is proportional to the prostaglandin tracer bound to the well and inversely to the amount present in the well during incubation. In comparisons of tested compounds to various controlled incubations, the percentage inhibition was measured. The concentration-response curve was plotted for the calculation of the concentration of test compounds that give IC_{50} μM (COX-II).

Table 6: The IC_{50} values of the synthetic compounds against COX-I/COX-II

Compounds	**COX-1 IC50 (μM)**	**COX-2 IC50 (μM)**
KRM-A	>1000	>1000
KRM-B	0.114±0.005	0.165±0.007
KRM-C	>100	>1000
KRM-D	0.091±0.003	0.134±0.006
KRM-E	0.185±0.008	>100
KRM-F	0.310±0.014	0.119±0.005
KRM-G	1.140±0.050	>100
KRM-H	>100	0.228±0.010
KRM-J	2.051±0.090	>100
KRM-K	0.415±0.020	1.526±0.060
KRM-L	>100	>1000
SC560	0.006± 0.0002	-
Ibuprofen	2.450±0.135	5.326±0.218
Celecoxib		0.132±0.005
Nimesulide		1.684±0.079

Most chemical structures are three-membered rings for COX-II inhibitors on the central amide group as spacers between the aryl and benzyl groups. The new COX-II inhibitors can reduce irritation or ulceration due to the different structural modifications of existing synthetic new compounds with different anti-inflammatory activity [28, 29].

The compounds Band D exhibited potent COX-II inhibited with IC_{50} of 0.134±0.006 and

0.165±0.007μmole/L, while compounds F, D, B, and H have significant anti-inflammatory activity greater than the celecoxib (reference) (Table 6).

However, the results indicate the electronic, shape and spatial of these synthetic compounds govern the COX-II enzyme inhibition and comply with the docking study. The order of the compound activity against COX-II enzyme is as follows: F > D > B > H with higher activity, the IC_{50} 0.119±0.005, 0.134±0.006, and 0.165±0.007, and 0.228±0.010 μmole/L respectively. Further studies will be conducted to enhance the activity and selectivity against COX-II coenzyme.

4. Conclusion

Employing density functional theory (DFT) for in silico studies, we estimated the electronic properties and reactivity of these compounds, while docking studies helped elucidate their potential binding interactions with biological targets. Furthermore, comprehensive in vitro evaluations revealed a spectrum of biological activities: antimicrobial, antioxidant, anticancer, and anti-inflammatory effects were systematically screened. Among these diverse bioactivities, several compounds exhibited significant inhibitory effects on cyclooxygenase enzymes COX-I and COX-II, suggesting their potential as potent anti-inflammatory agents. These findings not only demonstrate the versatility and efficacy of this synthetic approach but also emphasize the therapeutic potential of 2-(2-aryl amino) phenyl acetamide derivatives across multiple domains of medical science.

Acknowledgements: The authors sincerely thank the College of Pharmacy, Duhok University for their assistance.

Conflicts of Interest: The authors declare no conflict of interest.

References

1. Hassan G.S., Rahman D.E., Abdelmajeed E.A., Refaey R.H., Salem M.A., Nissan Y.M. New pyrazole derivatives: Synthesis, anti-inflammatory activity, cycloxygenase inhibition assay and evaluation of mPGES // European journal of medicinal chemistry, 2019, V.171, p. 332-42.
2. Abdellatif K.R.A., Abdelall E.K.A., Bakr R.B. Nitric oxide-NASIDS donor prodrugs as hybrid safe anti-inflammatory agents // Current topics in medicinal chemistry, 2017, V. 17(8), p. 941-55.
3. El-Sayed N.A., Nour M.S., Salem M.A., Arafa R.K. New oxadiazoles with selective-COX-2 and EGFR dual inhibitory activity: Design, synthesis, cytotoxicity evaluation and in silico studies // European Journal of Medicinal Chemistry, 2019, V.183, 111693.
4. Asirvatham S., Dhokchawle B.V., Tauro S.J. Quantitative structure activity relationships studies of non-steroidal anti-inflammatory drugs: A review // Arabian Journal of Chemistry, 2019, V.12(8), p. 3948-62.
5. Jakiela B., Soja J., Sladek K., Przybyszowski M., Plutecka H., Gielicz A., Rebane A., Bochenek G. Heterogeneity of lower airway inflammation in patients with NSAID-exacerbated respiratory disease // Journal of Allergy and Clinical Immunology, 2021, V. 147(4), p. 1269-80.
6. Mabrouk A.A., Tadros M.I., El-Refaie W.M. Improving the efficacy of Cyclooxegenase-2 inhibitors in the management of oral cancer: Insights into the implementation of nanotechnology and mucoadhesion // Journal of Drug Delivery Science and Technology, 2021, V.61, 102240.
7. Libby P., Hansson G.K. From focal lipid storage to systemic inflammation: JACC review topic of the week // Journal of the American College of Cardiology, 2019, V. 74(12), p. 1594-607.

8. Zhang M., Xia F., Xia S., Zhou W., Zhang Y., Han X., Zhao K., Feng L., Dong R., Tian D., Yu Y. NSAID-associated small intestinal injury: an overview from animal model development to pathogenesis, treatment, and prevention // Frontiers in Pharmacology, 2022, V. 13, 818877.
9. Khalil R.A., Abdulrahman S.A. Newly developed statistically intensive QSAR models for biological activity of isatin derivatives // Studia Universitatis Babes-Bolyai, Chemia, 2022, V. 67(1), V. 139-52.
10. Khalil R., Shayma'a H.A. A Developed QSPR Model for the Melting Points of Isatin Derivatives // Turkish Computational and Theoretical Chemistry, 2022, V. 6(1), p. 1-8.
11. Hantoush A., Najim Z., Abachi F. Density functional theory, ADME and docking studies of some tetrahydropyrimidine-5-carboxylate derivatives // Eurasian Chemical Communications, 2022, V. 4, p. 778-89.
12. Basit A., Ahmad S., Naeem A., Usman M., Ahmed I., Shahzad M.N. Chemical profiling of Justicia vahlii Roth. (Acanthaceae) using UPLC-QTOF-MS and GC-MS analysis and evaluation of acute oral toxicity, antineuropathic and antioxidant activities // Journal of Ethnopharmacology, 2022, V. 287, 114942.
13. Mahmood S., Khan S.G., Rasul A., Christensen J.B., Abourehab M.A. Ultrasound Assisted Synthesis and In Silico Modelling of 1, 2, 4-Triazole Coupled Acetamide Derivatives of 2-(4-Isobutyl phenyl) propanoic acid as Potential Anticancer Agents // Molecules, 2022, V. 27(22), 7984.
14. Sridhar K., Charles A.L. In vitro antioxidant activity of Kyoho grape extracts in DPPH and ABTS assays: Estimation methods for EC50 using advanced statistical programs // Food Chemistry, 2019, V. 275, p. 41-9.
15. Cooper M.A., Shlaes D. Fix the antibiotics pipeline // Nature, 2011, V. 472(32), 7341
16. Payne D.J., Gwynn M.N., Holmes D.J., Pompliano D.L. Drugs for bad bugs: confronting the challenges of antibacterial discovery // Nature reviews Drug discovery, 2007, V. 6(1), p. 29-40.
17. Graves N., Halton K., Paterson D., Whitby M. Economic rationale for infection control in Australian hospitals // Healthcare infection, 2009, V. 14(3), p. 81-8.
18. Hopwood D., Levy S., Wenzel R.P., Georgopapadakou N., Baltz R.H., Bhavnani S., Cox E. A call to arms // Nature, 2007, No. 6, p. 8-12.
19. Davies D.S. Annual Report of the Chief Medical Officer: Infections and the rise of antibiotic resistance // Infections and the rise of antibiotic resistance, Chpt 11: Future Challenges, 2013,
20. Bassetti M., Ginocchio F., Mikulska M. New treatment options against gram-negative organisms // Critical Care, 2011, V. 15(2), p. 215.
21. Krushkal J., Negi S., Yee L.M., Evans J.R., Grkovic T., Palmisano A., Fang J., Sankaran H, McShane L.M., Zhao Y., O'Keefe B.R. Molecular genomic features associated with in vitro response of the NCI-60 cancer cell line panel to natural products // Molecular Oncology, 2021, V. 15(2), p. 381-406.
22. Monks A., Zhao Y., Hose C., Hamed H., Krushkal J., Fang J., Sonkin D., Palmisano A., Polley E.C., Fogli L.K., Konaté M.M. The NCI transcriptional pharmacodynamics workbench: a tool to examine dynamic expression profiling of therapeutic response in the NCI-60 cell line panel // Cancer research, 2018, V. 78(24), p. 6807-17.
23. Dancey J.E., Chen H.X. Strategies for optimizing combinations of molecularly targeted anticancer agents // Nature reviews Drug discovery, 2006, V.5(8), p. 649-59.
24. Holbeck S.L. Update on NCI in vitro drug screen utilities // European Journal of Cancer, 2004, V. 40(6), p. 785-93.
25. Kazakova O., Șoica C., Babaev M., Petrova A., Khusnutdinova E., Poptsov A., Macașoi I., Drăghici G., Avram Ș., Vlaia L., Mioc A. 3-Pyridinylidene derivatives of chemically modified lupane and ursane triterpenes as promising anticancer agents by targeting apoptosis // International Journal of Molecular Sciences, 2021, V. 22(19), 10695.
26. Siegel R.L., Miller K.D., Jemal A. Cancer statistics, 2018. CA // a cancer journal for clinicians, 2018, V. 68(1), p. 7-30.
27. Madhava G., Ramana K.V., Sudhana S.M., Rao D.S., Kumar K.H., Lokanatha V., Rani A.U., Raju C.N. Aryl/heteroaryl substituted

celecoxib derivatives as COX-2 inhibitors: Synthesis, anti-inflammatory activity and molecular docking studies // Medicinal Chemistry, 2017, V.13(5), p. 484-97.
28. Ahmadi M., Bekeschus S., Weltmann K.D., von Woedtke T., Wende K. Non-steroidal anti-inflammatory drugs: Recent advances in the use of synthetic COX-2 inhibitors // RSC Medicinal Chemistry, 2022, V. 13(5), p. 471-96.
29. Boshra A.N., Abdu-Allah H.H., Mohammed A.F., Hayallah A.M. Click chemistry synthesis, biological evaluation and docking study of some novel 2′-hydroxychalcone-triazole hybrids as potent anti-inflammatory agents // Bioorganic chemistry, 2020, V.95, 103505.
30. Zhang Z., Ghosh A., Connolly P.J., King P., Wilde T., Wang J., Dong Y., Li X., Liao D., Chen H., Tian G. Gut-restricted selective cyclooxygenase-2 (COX-2) inhibitors for chemoprevention of colorectal cancer // Journal of Medicinal Chemistry, 2021, V.64(15), p. 11570-96.

BƏZİ 2-(2-ARİL AMİN) FENİLASETAMİD TÖRƏMƏLƏRİNİN SIXLIQ FUNKSİONAL NƏZƏRİYYƏSİ İLƏ TƏDQİQİ, DOKİNQİ, SİNTEZİ VƏ BİOLOJİ QİYMƏTLƏNDİRİLMƏSİ

Karam S. Atruşi[1], Dana M. Amin[1], Faris T. Abaçi[3]*

[1]Duhok Universiteti Əczaçılıq Kolleci, Əczaçılıq Kimyası Departamenti.
[2]Howler Tibb Universiteti, Əczaçılıq Kolleci, Əczaçılıq Kimyası Bölməsi, Ərbil.
[3]Əczaçılıq Departamenti, Əl-Hədba Universiteti Kolleci, Mosul, İraq.
e-mail: Faris_abachi@uomosul.edu.iq

Xülasə: Bir sıra yeni 2-(2-aril amin) fenilasetamid törəmələri sintez edilmiş və onların kimyəvi strukturları spektroskopik üsullardan (UV-VIS, FT-IR, ^{1}H-NMR və MS) istifadə edilərək müəyyənləşdirilmişdir. Asetamid törəmələri üçün proqnozlaşdırılan reaktivlik və sıxlıq funksiyası nəzəriyyəsi (DFT) hesablamaları üzrə tədqiqatlar aparılmış, həmçinin ən çox dolmuş və ən aşağı boşluqlu molekulyar orbitalın (ABMO) elektronlarının fəzada paylanması hesablanmışdır. Prostaglandin sintetaza-2 (COX-II koenzimi) əleyhinə dokinq tədqiqatı aparılmış və nəticədə dörd birləşmə üçün (D, F, H və L) yüksək göstəricilər (Kcal/mol) əldə edilmişdir. Bu sintetik birləşmələrin bəziləri *in vitro* (antimikrob, antioksidant, xərçəng və iltihab əleyhinə) bioloji fəaliyyətlərinə görə qiymətləndirilmişdir. Nəticədə müəyyən edilmişdir ki, B, D, F və K birləşmələri tsikloksigenaza inhibitorları kimi nəzəri, eksperimental tədqiqatlar və zəif və ya orta dərəcədə antimikrob, antioksidant və xərçəngə qarşı yaxşı korrelyasiyaya malikdir.
Açar sözləri: COX-II inhibitorları, DFT, xərçəng əleyhinə, İOMO, Asetamid törəmələri.

ТЕОРИЯ ФУНКЦИОНАЛА ПЛОТНОСТИ, ДОКИНГ, СИНТЕЗ И БИОЛОГИЧЕСКАЯ ОЦЕНКА НЕКОТОРЫХ ПРОИЗВОДНЫХ 2-(2-АРИЛАМИНО)ФЕНИЛАЦЕТАМИДА

Карам С. Атруши[1], Дана М. Амин[2], Фарис Т. Абачи[3]*

[1]Кафедра фармацевтической химии, Фармацевтический колледж, Университет Духока.
[2]Кафедра фармацевтической химии, Фармацевтический колледж, Медицинский университет Хоулера, Эрбиль.
[3]Фармацевтический факультет Университетского колледжа Аль-Хадбаа, Мосул, Ирак
e-mail: Faris_abachi@uomosul.edu.iq

Резюме: Синтезирован ряд новых производных 2-(2-ариламино)фенилацетамида и идентифицирована их химическая структура с использованием спектроскопических методов (УФ, ИК, ^{1}Н-ЯМР и МС). Были проведены вычислительные исследования для прогнозирования реакционной способности и расчета теории функционала плотности (ТФП) для производных ацетамида, а также было рассчитано пространственное распределение электронов высшей занятой молекулярной орбитали (ВЗМО) и нижней незанятой молекулярной орбитали (ННМО). Было проведено расчетное исследование стыковки с простагландинсинтетазой-2 (коэнзим ЦОГ-II), и четыре соединения (D, F, H и L) дали высокие оценки (ккал/моль). Некоторые из этих синтетических соединений были оценены на предмет их биологической активности *in vitro* (противомикробная, антиоксидантная, противораковая и противовоспалительная). Наконец, соединения B, D, F и K имеют хорошую корреляцию между теоретическими и экспериментальными исследованиями в качестве ингибиторов циклооксигеназы и обладают противомикробной, антиоксидантной и противораковой активностью от слабой до умеренной.

Ключевые слова: ингибиторы COX-II, теория функционала плотности (ТФП), противораковые препараты, ВЗМО, производные ацетамида.